①

Interaction Notes

Note 440

June 1984

Creeping Ray Analysis of Resonance
For Prolate Spheroid

A. Q. Howard, Jr., R. M. Jones, J. I. Simon
Department of Electrical & Computer Engineering
University of Arizona
Tucson, Arizona   85721

89   6 29   007

89 6 27 502

CREEPING RAY ANALYSIS OF RESONANCE
FOR PROLATE SPHEROID

Abstract -- A ray orbit resonance condition is postulated and shown
to reproduce asymptotically the resonant frequencies of a prolate spheroid.
The method uses local creeping rays associated with a smooth convex
impedance surface. As expected, the method deteriorates for high aspect
ratio spheroids where the tip radii of curvatures are electrically
small. This work is an alternative approach to Howard's earlier geometric
treatment and gives the relation to creeping ray analysis. The theory
provides impetus to the understanding of mode conversion and diffraction
ray coupling near edges of such scatterers. Comparison of pole location,
pole trajectories and layering with L. Marin's analysis (1972) is given.

I. INTRODUCTION

There continues to be strong interest in the singularity expansion
method (SEM) and its application to the radar target identification problem.
The singularities are the complex resonant frequencies in the ω or s-plane
and exist in layers. Resonance requires at least one orbit of a ray and,
therefore, for the external problem, the radiation loss, associated with
the imaginary part of the frequency, is considerable. Thus, the resonance

poles describe relatively late times of a low Q resonator. This is a difficult regime for the object identification problem. For this translates to small signal amplitudes and, hence, poor signal to noise levels. In addition, the required signal processing is non-linear and it happens that small errors in the signal can result in large errors in pole location [1]. To attempt to overcome these difficulties, one can take advantage of the redundant information associated with pole layering. Thus, identification can be based upon pole families, not individual poles. This requires theoretical understanding and prediction of the ordering of the higher order pole locations.

This is precisely the high frequency regime where asymptotic geometrical methods apply. Indeed, just as classical mechanics is asymptotic to quantum mechanics in the limit of large quantum numbers, so our asymptotic theory applies as the discrete complex frequency index becomes large. Our geometric method also requires the local radius of curvature to be large with respect to a wavelength.

In a previous paper by one of us [2], the method of Keller and Rubinow [3] was extended to the exterior resonance problem. In this paper, we make explicit use of the creeping ray condition (see equation 1), while in the previous paper [2], the equivalent effect was developed using an additional explicit radial resonance condition. This additional condition inforced transverse resonance between the surface of the scattering object and a turning point caustic.

Recently, Heyman and Felsen have also shown, using a method having some similarities with ours, that local creeping rays describe exterior resonances on smooth convex objects [4].

II. THEORY

We make free use of the comprehensive results of Bremmer [5], Fock [6], Wait [7], Logan [8], and more recently D. S. Jones [9]. In these references, it is shown that the creeping wave mode equation for a cylinder of radius ρ, and for vertically polarized waves, is

$$\frac{1}{k} \frac{H_\nu^{(1)'}(k\rho)}{H_\nu^{(1)}(k\rho)} - \frac{1}{k_1} \frac{H_\nu^{(2)'}(k_1\rho)}{H_\nu^{(2)}(k_1\rho)} = 0 \tag{1}$$

In equation (1), $H_\nu^{(j)}(z)$ is the Hankel function of order ν and argument z of type j (j is 1 or 2). For a fixed frequency ω, equation (1) has a discrete set of roots ν_s, $s = 1, 2, 3 \ldots$. We are using the time dependence $e^{-i\omega t}$. Here, $k = \omega/c$ is the wave number of free space and k_1 is the complex wave number of the spheroid. Condition (1) has the physical interpretation that the surface reflection coefficient is infinite. This allows a reflected wave with no incident wave which is a condition of resonance.

The propagation along the spheroid surface has angular dependence

$$\exp(i\nu\alpha) \tag{2}$$

where α is an angular distance along the surface. In our application, we allow ρ in equation (1) to be a variable. In this ray treatment, ρ is the local radius of curvature of the spheroid along the direction of the ray path. Hence, it is a continuous function of position. Only the radius of curvature in the direction of propagation is significant. The transverse curvature is insignificant. We know that because the local ground wave modes for a sphere and cylinder of the same radius and material are equal.

5

The asymptotic creeping ray resonance condition is given by

$$\oint \nu \, d\theta = 2\pi(n + \frac{1}{2})$$

(3)

The term $\nu \, d\theta$ is the incremental complex phase advance where $d\theta = \frac{ds}{\rho}$, and where ds is the arc length along spheroid and ρ is the local radius of curvature. The additional phase of π corresponds to the phase shift advance of $\pi/2$ going through the focus at each tip of the spheroid. Details of this shift are given in the appendix.

There are two geodesic paths on a spheroid. First, there is the path from one tip of the spheroid to the other; there is a continuum of these. They cross at the tips which give rise to the focus phase shift. Second, the path going around the equator; the resonances for this second path are easier to calculate because they are the same as the sphere.

Returning to (3), along the ray path implicit in the closed path integral, we can consider the geometry as two dimensional. Along such a ray let the surface be represented as

$$y = f(x)$$

(4)

Then it follows from elementary differential geometry [10] that

$$d\theta = \frac{ds}{\rho} = [f''(x)/(1 + (f'(x))^2)] \, dx$$

(5)

Let us apply this to an elliptic cross section of a prolate spheroid for principal orbit planes containing the axis of revolution. Then

$$f(x) = \pm (b^2 - c^2 x^2)^{\frac{1}{2}}$$

(6)

where $c = b/a \leq 1$ is the aspect ratio of the ellipse and where a and b are

6

the semi-major and semi-minor axes. Substitution of (6) into (5) yields

$$d\theta = [b^2c^2/((b^2-c^2\alpha^2x^2)(b^2-c^2x^2))]\,dx \qquad (7)$$

where

$$\alpha^2 = 1 - c^2$$

The resonance condition (3) depends upon the propagation constant ν. The propagation constant ν in turn depends upon the local radius of curvature ρ which for the elliptic surface is given by

$$\rho = (1 + (f'(x))^2)^{3/2}/f''(x) = (b^2 - c^2\alpha^2x^2)^{3/2}/(c^2b^2) \qquad (8)$$

In view of the dependence of the creeping ray propagation constant ν on the local parameter $k\rho$, as given by equation (1), it is useful to make a further change of integration variable

$$\tau^3 = c^2\rho/b \qquad (9)$$

Then the resonance condition (3) becomes

$$c\int_c^1 \frac{\nu\,d\tau}{\tau(\tau^2-c^2)^{\frac{1}{2}}(1-\tau^2)^{\frac{1}{2}}} = (n+\tfrac{1}{2})\,\pi/2 \qquad (10)$$

In (10) we have accounted for the four fold symmetry of the orbit. Note that the integrand in (10) is singular at both end points $\tau = c$ and 1. These singularities are removable. Thus, we make the linear change of variable

$$\tau = \frac{1+c}{2} + \frac{1-c}{2}\,x \qquad (11)$$

to obtain

$$\frac{2}{1-c} \int_{-1}^{+1} \frac{g(\frac{1+c}{2} + \frac{1-c}{2} x)}{(1-x^2)^{\frac{1}{2}}} \, dx = 2\pi(n+\frac{1}{2}) \tag{12}$$

where

$$g(u) = \frac{4c \, \nu(u)}{u(u+c)^{\frac{1}{2}} (1+u)^{\frac{1}{2}}} \tag{13}$$

is nonsingular.

Now we make the further change of variables

$$x = \sin \pi/2 \, s$$

Then (12) becomes

$$\frac{\pi}{1-c} \int_{-1}^{+1} g(\frac{1+c}{2} + \frac{1-c}{2} \sin(\frac{\pi}{2} s)) \, ds = 2\pi(n+\frac{1}{2}) \tag{14}$$

This form is suitable for numerical integration.

III. SOME APPROXIMATIONS

In the high frequency limit, the creeping ray condition (1) can be simplified. The relevent approximations are discussed in detail in several references ([5], [6], [7], [8]).

A more modern mathematical treatment is given by Olver [11]. Olver derives a uniform asymptotic expansion which assumes the argument and order are large and approximately equal. The uniform asymptotic expansion is given in terms of Airy functions. The lead term in the expansion is given by

8

$$H_{\nu}^{(1)} (z\nu) \cong \frac{2e^{-i\pi/3}}{\nu^{1/3}} \left(\frac{4b}{1-z^2}\right)^{1/4} A_i(\nu^{2/3} \zeta \omega) \tag{15}$$

where

$$2/3\, \zeta^{3/2} = -\int_1^z (1-t^2)^{1/2}/t\, dt, \quad \omega = \exp(i2\pi/3) \tag{16}$$

The phase factor $\omega = \exp(i2\pi/3)$ is common in these approximations. In fact, Fock defined his $W_1(z)$ function as,

$$W_1(z) = -2\omega\, i\, \omega^{\frac{1}{2}} A_i(\omega z) \tag{17}$$

This function is outward radiating at infinity. The implicit relation (16) can be expanded as a function of ζ. The expansion needed is around $z \approx 1$ and hence $\zeta \approx 0$. One determines

$$z(\zeta) = 1 - 2^{-1/3}\zeta + 3/10 2^{-2/3} \zeta^2 + 1/700\, \zeta^3 + \ldots \tag{18}$$

Series (18) can be manipulated (under the same conditions required to produce (8)) to yield the information

$$\nu = k\rho + \left(\frac{k\rho}{z}\right)^{1/3} t + \frac{1}{60} \left(\frac{2}{k\rho}\right)^{1/3} t^2 + \ldots \tag{19}$$

where $t = \nu^{2/3} \zeta$ and it is assumed $k\rho \gg 1$. In addition, series (18) can also be used to obtain the expansion

$$\zeta = 2^{1/3} \left[(1-z) + \frac{3}{10}(1-z)^2 + \ldots \right. \tag{20}$$

$$z = k\rho/\nu$$

Also from (15) and (17) we determine

$$H^{(1)}_\nu (k\rho) \cong 2e^{-i\,\pi/2}\,\nu^{-1/3}\,\left(\frac{4\zeta}{1-z^2}\right)^{1/4} W_1(t)$$

where for $z \cong 1$, to first order, this reduces to

$$H^{(1)}_\nu (k\rho) \cong 2^{4/3}\,e^{-i\,\pi/2}\,\nu^{-1/3}\,W_1(t) \tag{21}$$

An explicit representation of the Fock function $W_1(t)$ is

$$W_1(t) = \frac{1}{\pi^{\frac{1}{2}}} \int_{\infty\omega^*}^{\infty} \exp(st - s^3/3)\, ds \tag{22}$$

where

$$\omega^* = \exp(-i\,2\pi/3)$$

This integral has two first order saddle to points at $s_{s.p.} = \pm\sqrt{t}$ which coalesce at $t = 0$. The coalescence corresponds to the position of the creeping ray caustic.

It remains to determine an asymptotic ray approximation to the modal equation (1).

IV. IMPEDANCE BOUNDARY CONDITION

At high frequencies, and when the object to which the creeping ray attaches is convex and a relatively good conductor, it is not necessary to compute the fields on the inside of the object. This is possible because under these conditions, the fields inside are geometrical and propagate nearly normal to the surface. The ratio of tangential $\overline{E}$ and $\overline{H}$ is approximately the same as for a plane wave. The general formulation is known as the Leontovich boundary condition and a good account is by this original

10

author [12]. From this discussion it follows that the normal surface wave
impedance $z_n^{(1)}$ in the limit from inside is given by

$$z_n^{(1)} = \begin{cases} z_0 k / \sqrt{k_1^2 - k^2} & \text{, horizontal polarization} \\ \\ z_1 \sqrt{k_1^2 - k^2} / k_1 & \text{, vertical polarization} \end{cases} \qquad (23)$$

The terminology is with respect to the electric vector. Thus, horizontal
corresponds to the electric vector in the plane of the surface, vertical
corresponds to $\bar{H}$ lying in the plane of the local surface. The intrinsic
wave number k_1 is complex, i.e.

$$k_1 = \omega \sqrt{\mu_0 \tilde{\varepsilon}_1} \; , \; \tilde{\varepsilon}_1 = \varepsilon_1 + i \sigma / \omega \qquad (24)$$

$$\text{Im}(k_1) \geq 0.$$

The wave impedance (23) is a ratio of tangential components at the surface
of the scatterer. Hence, the corresponding ratio on the exterior has the
same limiting value.

$$z_n = z_n^{(1)} \qquad (25)$$

On the exterior, it follows from Maxwell's equations that

$$z_n = \begin{cases} i \omega \mu_0 \, \psi / \frac{\partial \psi}{\partial n} & \text{, horizontal} \\ \\ \frac{\partial \psi}{\partial n} / (i \omega \varepsilon \psi) & \text{, vertical} \end{cases} \qquad (26)$$

Substitute (26) into (25). Let ψ and $\frac{\partial \psi}{\partial n}$ be the tangential E or H field for

horizontal or vertical polarization, where $\partial/\partial n$ is the outward pointing normal derivative. Then, the Leontovich boundary condition is explicitly given by

$$\frac{\partial \psi}{\partial n} + \Delta \psi = 0 \tag{27}$$

where

$$\Delta = \begin{cases} -i \sqrt{k_1^2 - k^2} & \text{, horizontal polarization} \\ \\ -i k^2 \sqrt{k_1^2 - k^2} / k_1^2 & \text{, vertical polarization} \end{cases}$$

We now relate this development of the homogeneous boundary condition (27) to our creeping ray analysis.

Recall that in equation (8) we have defined ρ to be the local radius of curvature of the object along the creeping ray path direction. Thus, the normal derivative $\partial/\partial n = \partial/\partial \rho$. Then, using (21) and (27) yields the explicit modal equation

$$w_1'(t) - q w_1(t) = 0 \tag{28}$$

where the normalized impedance parameter q is given by

$$q = -i (\nu/2)^{1/3} \sqrt{k_1^2 - k^2} \begin{cases} 1/k, \text{ horizontal polarization} \\ \\ k/k_1^2, \text{ vertical polarization} \end{cases} \tag{29}$$

In the perfectly conducting limit, the modal equation further simplifies to

$w_1(t_m) = C$ horizontal polarization

$w_1'(t_m') = 0$ vertical polarization   (30)

$m = 1, 2, 3 \ldots$

The roots t_m and t_m' for $w_1(t) = 0$ and $w_1'(t) = 0$ respectively are related to the roots of the Airy function Ai by relation (17). The Airy function has isolated zeros along the negative real axis. There are no others. Thus, the roots defined by (30) all lie on the ray $e^{i\,4\pi/3}$ i.e.

$$t_m = e^{i\,4\pi/3}\, a_m$$

$$t_s' = e^{i\,4\pi/3}\, a_m' \hspace{3cm} (31)$$

Abramowitz and Stegun have listed the first ten of them [13]. They are:

m	a_m	a_m'
1	-2.33810741	-1.01879297
2	-4.08794944	-3.24819758
3	-5.52055983	-4.82009921
4	-6.78670809	-6.16330736
5	-7.9413359	-7.37217726
6	-9.02265085	-8.48848673
7	-10.04017434	-9.53544905
8	-11.00852430	-10.52766040
9	-11.93601556	-11.47505663
10	-12.82877676	-12.38478837

Table 1: Zeros of Ai(z) and Ai'(z)
(from Abramowitz and Stegun, p. 478)

Asymptotically for large m, the zeros a_m and a_m' are given by

$$a_m = -(3\pi(4m - 1)/8)^{2/3} + 0\,(m^{-4/3})$$

$$a_m' = -(3\pi(4m - 3)/8)^{2/3} + 0\,(m^{-4/3}) \hspace{2cm} (32)$$

If the surface is not perfectly conducting, mode equation (28) must be solved. However, Airy's differential equation for $W_1(t)$ is

$$W_1''(t) - t\,W_1(t) = 0 \tag{33}$$

This can be checked, i.e. $W_1(t)$ as defined by equation (22) satisfies (33). Thus, the roots t_s as a function of q satisfy the differential equation.

$$\frac{d\,t_m}{dq} = \frac{1}{t_m - q^2} \tag{34}$$

This is a nonlinear Riccati equation which has been solved in the Bremmer reference [6].

V. ASYMPTOTIC SOLUTION OF RESONANT FREQUENCIES

Given the angular propagation constant ν, (equation (19)), the resonance condition (10) becomes

$$\left(n + \frac{1}{2}\right) \frac{\pi}{2} = ka \int_c^1 \frac{\tau^2\, d\tau}{\left((1 - \tau^2)(\tau^2 - c^2)\right)^{\frac{1}{2}}}$$

$$+ c^{2/3} \left(\frac{ka}{2}\right)^{1/3} t_m \int_c^1 \frac{d\tau}{\left((1 - \tau^2)(\tau^2 - c^2)\right)^{\frac{1}{2}}}$$

$$+ \frac{c^{4/3} t_m^2}{60} \left(\frac{2}{ka}\right)^{1/3} \int_c^1 \frac{d\tau}{\tau^2 \left((1 - \tau^2)^{\frac{1}{2}} (\tau^2 - c^2)\right)^{\frac{1}{2}}} \tag{35}$$

The integrals on the right hand side of (35) are tabulated special functions.

14

The first is k/4 times the perimeter of an ellipse (reference [14], # 223.6c, p. 49) i.e.

$$\int_c^1 \frac{\tau^2 \, d\tau}{\left((1-\tau^2)^{\frac{1}{2}}(\tau^2-c^2)\right)^{\frac{1}{2}}} = E(\sqrt{1-c^2})$$

where

$$E(x) = \int_0^{\pi/2} (1-x^2 \sin^2\theta)^{\frac{1}{2}} \, d\theta \qquad \cdot \qquad \qquad (36)$$

is a complete elliptic integral of the second kind (references [13] p. 590, and [15]).

Result (36) follows from the change of variable $x = \left((1-\tau^2)/(1-c^2)\right)^{\frac{1}{2}}$ and then the subsequent change of integration variable $\sin\theta = x$. Similar changes of variables can be made to determine

$$\int_c^1 \frac{d\tau}{\left((1-\tau^2)(\tau^2-c^2)\right)^{\frac{1}{2}}} = \frac{2}{1+c} \, K\left(\frac{1-c}{1+c}\right)$$

where

$$K(x) = \int_0^{\pi/2} (1-x^2 \sin^2\theta)^{-\frac{1}{2}} \, d\theta \qquad \qquad (37)$$

The K function is the complete elliptic integral of the third kind given also by Abramowitz and Stegun [13]. The same substitutions used in obtaining (36), and when an additional substitution $\tau' = \frac{1}{\tau}$ leads to the result

$$\int_c^1 \frac{d\tau}{\tau^2\left((1-\tau^2)(\tau^2-c^2)\right)^{\frac{1}{2}}} = \frac{1}{c^2} E(\sqrt{1-c^2}) \qquad \qquad (38)$$

15

Mode equation (35) thus becomes

$$x^3 + \frac{c^{2/3}}{1+c} \frac{K(\frac{1-c}{1+c})}{E\left(\sqrt{1-c^2}\right)} t_m x - \frac{(n+\frac{1}{2})\pi}{4E\left(\sqrt{1-c^2}\right)} + \frac{t_m^2 c^{-2/3}}{120x} = 0 \qquad (39)$$

where $x = (ka/2)^{1/3}$.

Thus, (39) is a quartic equation in x with complex coefficients. In the perfectly conducting limit, from (31) it is seen that t^3 is real. This suggests the change of variable.

$$x = y \, t_m^2$$

Then (39) becomes

$$y^3 + \frac{c^{2/3}}{1+c} \frac{K(\frac{1-c}{1+c}) \, y}{E(\sqrt{1-c^2}) \, t_m^3} - \frac{(n+\frac{1}{2}) \, \pi}{4E(\sqrt{1-c^2} \, t_m^6} + \frac{c^{-2/3}}{120 \, t_m^6 \, y} = 0 \qquad (40)$$

Notice the coefficients in (40) in the perfectly conducting limit are real. The complex normalized frequency

$$\Omega_{nm} = k \, a \qquad , n, m = 1,2,3 \ldots$$

depends upon two integers, n and m, which order the roots in the angular (θ) and radial (ρ) coordinates. In the terminology of Marin [16],

$$\gamma_{nm} = -i k_{nm} = -\frac{i\omega_{nm}}{c} = \frac{s_{nm}}{c} \qquad (41)$$

where here and what follows $c = 2.997925 \times 10^8$ m/sec and where ω_{ns} is the complex natural resonant frequency in radians/second, and s_{nm} is the Laplace transform pole location. In the figures to follow it is convenient

16

to plot the location of the unitless frequency

$$\gamma_{nm}a = \frac{s_{nm}a}{c} \qquad (42)$$

where a is the semi-major axis of the prolate spheroid.

Of course, since the actual electromagnetic time domain response must be real and causal, the poles in the complex s plane (or γa plane) must either lie on the negative axis or appear as complex conjugate pairs in the second and third quadrants. We, therefore, only plot results in the second quadrant.

VI. NUMERICAL RESULTS

In figure 1, we reproduce (from reference (16)) a pole trajectory of the first two pole layers of the prolate spheroid. Each curved line segment traces the motion of the poles in the second quadrant of the normalized s plane as the aspect ratio c = b/a varies from .1 to 1. Figures 2a through 2d are comparison plots of Marin's numerical solution of an integral equation [16] and ours. As would be expected of an asymptotic method, in the case of a sphere (figure 2a), the accuracy of our method is good. When the aspect ratio c = b/a departs from unity, the accuracy degrades since then at the tips of the prolate spheroid the radius of curvature becomes electrically small. This violates the asymptotic assumption. The second layer plotted further to the left in figures 2a through 2d correspond to m = 2 in the ray equation (40). The comparison is somewhat misleading as tables 2a through 2d show. The tables have the same information as the figures but, in addition, include the absolute relate error in percent entry in the fifth column.

The errors for m = 1 and m = 2 pole layers are seen to be comparable. Also, in these tables, it is evident that the accuracy improves as the
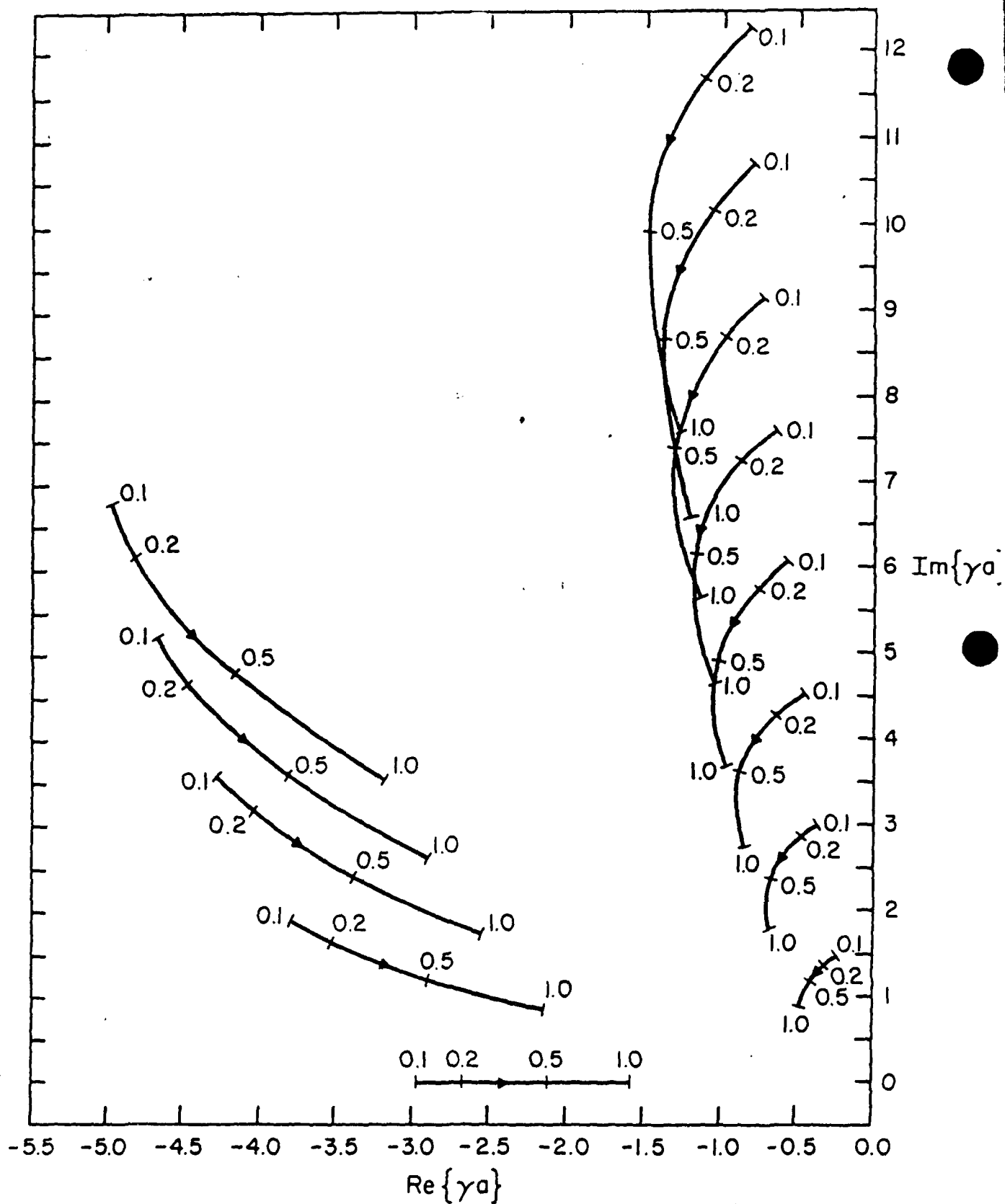
17

Fig. 1 The locus of natural frequencies when $0.1 \le b/a \le 1.0$. The location of the natural frequencies for $b/a = 0.1, 0.2, 0.5, 1.0$ is indicated on the curves. The arrow indicates the direction in which the natural frequencies move for increasing values of b/a. (After L. Marin, 1972.)
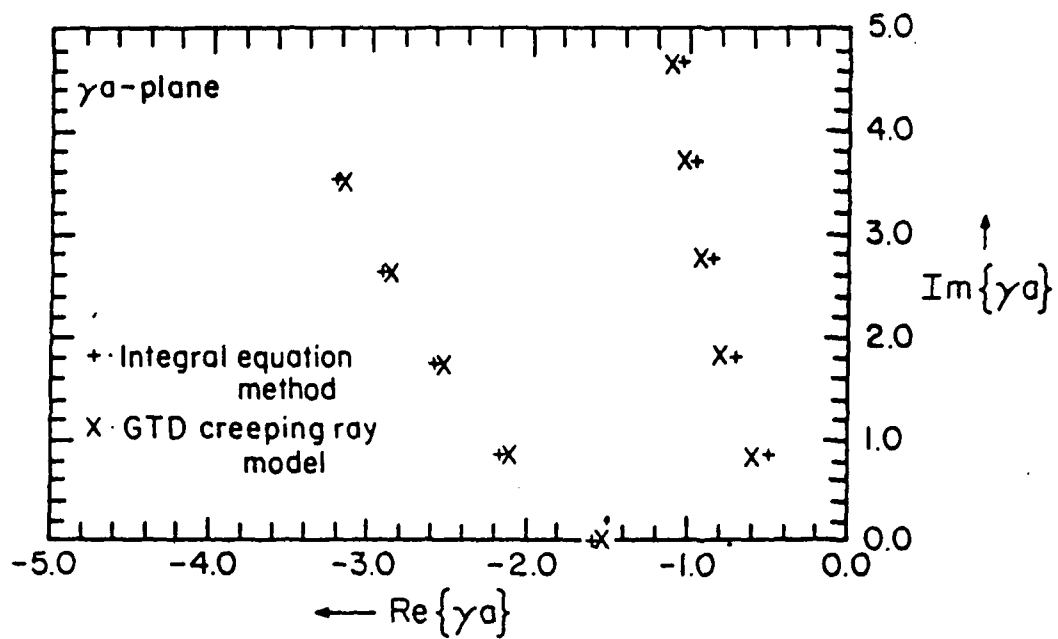
18

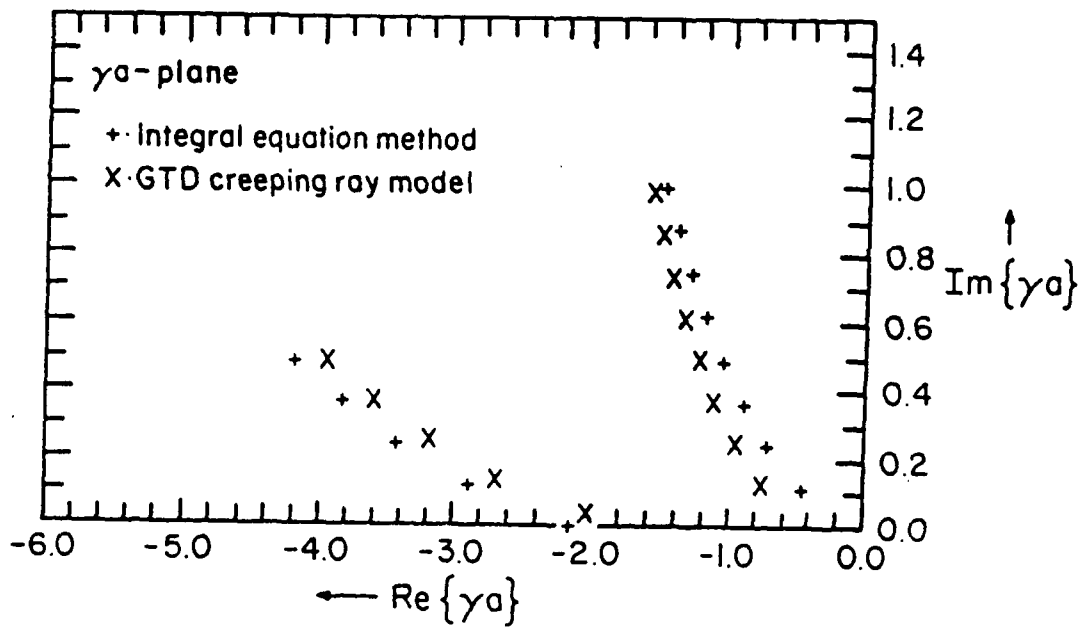Fig. 2a Natural frequencies of a prolate spheroid with b/a = 1.0

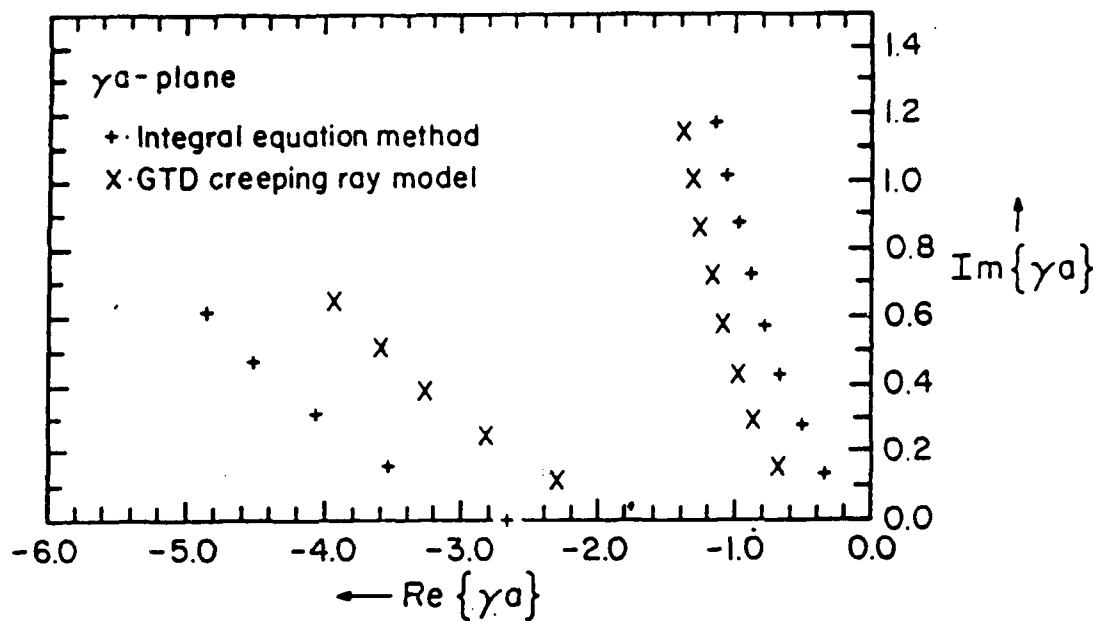Fig. 2b Natural frequencies of a prolate spheroid with b/a = 0.5

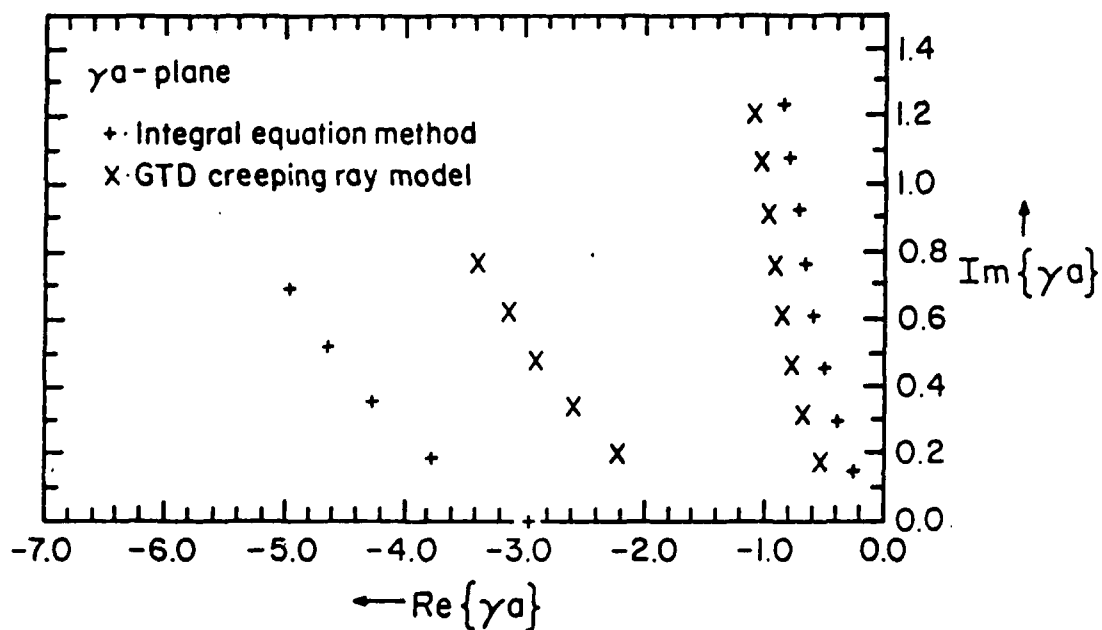Fig. 2c Natural frequencies of a prolate spheroid with b/a = 0.2

Fig. 2d Natural frequencies of a prolate spheroid with b/a = 0.1

Natural Frequencies of Prolate Spheroids

m	n	b/a = 1.0				
		Integral Equation Method		GTD Creeping Ray Solution		Absolute Relative Error (percent)
		Re$\{\gamma a\}$	Im$\{\gamma a\}$	Re$\{\gamma a\}$	Im$\{\gamma a\}$	
1	1	- .500	.866	- .622	.931	13.82
	2	- .702	1.807	- .795	1.851	5.31
	3	- .843	2.758	- .921	2.789	2.91
	4	- .954	3.715	-1.022	3.737	1.86
	5	-1.048	4.676	-1.108	4.692	1.30
	6	-1.129	5.642	-1.184	5.652	0.97
	7	-1.201	6.610	-1.251	6.615	0.75
	8	-1.267	7.580	-1.313	7.581	0.60
2	1	-1.596	0	-1.528	.007	4.28
	2	-2.157	.871	-2.105	.867	2.24
	3	-2.571	1.752	-2.525	1.744	1.50
	4	-2.908	2.644	-2.866	2.633	1.10
	5	-3.195	3.545	-3.156	3.532	0.86

Table 2a.   Mode Comparison for b/a = 1

m	n	b/a = 0.5				
		Integral Equation Method		GTD Creeping Ray Solution		Absolute Relative Error (percent)
		Re$\{\gamma a\}$	Im$\{\gamma a\}$	Re$\{\gamma a\}$	Im$\{\gamma a\}$	
1	1	- .453	1.152	- .745	1.232	24.46
	2	- .703	2.380	- .951	2.422	10.14
	3	- .890	3.623	-1.102	3.636	5.69
	4	-1.042	4.876	-1.222	4.863	3.62
	5	-1.171	6.136	-1.325	6.100	2.53
	6	-1.286	7.401	-1.415	7.343	1.88
	7	-1.388	8.669	-1.495	8.592	1.50
	8	-1.480	9.938	-1.569	9.844	0.94
2	1	-2.130	0	-2.017	.253	13.01
	2	-2.879	1.210	-2.687	1.372	8.04
	3	-3.408	2.410	-3.185	2.514	5.89
	4	-3.830	3.609	-3.591	3.672	4.70
	5	-4.187	4.810	-3.938	4.842	3.94

Table 2b.   Mode Comparison for b/a = 0.5

m	n'	b/a = 0.2				
		Integral Equation Method		GTD Creeping Ray Solution		Absolute Relative Error (percent)
		Re{γa}	Im{γa}	Re{γa}	Im{γa}	
1	1	- .336	1.374	- .674	1.548	26.88
	2	- .516	2.817	- .846	2.923	13.78
	3	- .655	4.277	- .973	4.326	7.44
	4	- .773	5.745	-1.075	5.745	5.21
	5	- .876	7.220	-1.162	7.175	3.98
	6	- .970	8.698	-1.239	8.612	3.23
	7	-1.057	10.180	-1.308	10.055	2.74
	8	-1.138	11.666	-1.370	11.502	2.42
2	1	-2.672	0	-2.312	1.194	46.67
	2	-3.522	1.652	-2.841	2.508	28.12
	3	-4.070	3.195	-3.252	3.847	20.22
	4	-4.491	4.694	-3.595	5.203	15.86
	5	-4.839	6.174	-3.892	6.573	13.10

Table 2c. Mode Comparison for b/a = 0.2

m	n	b/a = 0.1				
		Integral Equation Method		GTD Creeping Ray Solution		Absolute Relative Error (percent)
		Re{γa}	Im{γa}	Re{γa}	Im{γa}	
1	1	- .265	1.458	- .552	1.704	25.51
	2	- .400	2.977	- .678	3.136	10.61
	3	- .497	4.510	- .772	4.596	6.35
	4	- .582	6.051	- .848	6.071	4.39
	5	- .658	7.598	- .913	7.556	3.39
	6	- .727	9.149	- .971	9.047	2.88
	7	- .793	10.703	-1.022	10.545	2.59
	8	- .855	12.260	-1.069	12.046	2.46
2	1	-2.969	0	-2.226	1.990	71.55
	2	-3.776	1.886	-2.603	3.372	44.85
	3	-4.278	3.572	-2.904	4.779	32.77
	4	-4.660	5.194	-3.159	6.202	25.91
	5	-4.975	6.782	-3.382	7.639	21.51

Table 2d. Mode Comparison for b/a = 0.1

integer n increases. Thus, as also expected, our geometrical method improves as either ka or n increases.

VII. CONCLUSION

We have presented a geometrical creeping ray formulation of the natural oscillations of a prolate spheroid. The general formulation has obvious extensions to smooth rotationally symmetric convex objects. For aspect ratios not less than one half, the absolute percent error for all but the lower order (n = 1 and 2) pole locations is·less than 10%. As n increases, the error becomes less. At the tip of a prolate spheroid of aspect ratio $b/a = 0.1$ $|ka| = 10^{-3}$ so clearly asymptotic formulas such as (19), which are fundamental to this method, are inappropriate. In such cases, we recommend that tip diffraction be implemented. Indeed, the creeping rays loose their identity near such tips. In other words, strong "mode mixing" occurs. We will consider this addition to the theory in a future paper.

APPENDIX: PHASE ADVANCE AT TIP OF SPHEROID

At a focus, it is known that the phase of the converging rays experience a phase shift. Born and Wolf in their text [17] have a section on the three dimensional light distribution near a focus. Their model is a spherical wave emerging from a circular aperture and, hence conversely, converging on the opposite side of the aperture toward an axial focal point. Although geometrical optics predicts a discontinuous focus phase shift, finite wave length calculations show it to be continuous. For these optical treatments of phase behavior, the phase shift is π radians. As we shall now show this is not the same as for our problem. At the poles of a spheroid, the focus of creeping rays occur.

23

For a specific model, we choose a perfectly conducting spherical surface of radius a. For excitation, we use a vertical electric dipole. Sommerfeld gives a good derivation of this model [18]. After the Watson transformation, the potential u is determined to be

$$u(r,\theta)' = \frac{ik}{4} \sum_{\nu=\nu_0,\nu_1,\nu_2\cdots} \frac{2\nu+1}{\sin \nu\,\pi} P_\nu (-\cos\theta) \frac{h_\nu^{(1)}(kr)}{\eta_\nu(ka)} \tag{43}$$

In expression (43),

$$h_\nu^{(1)}(z) = (\pi/(2z))^{\frac{1}{2}} H_{\nu+\frac{1}{2}}^{(1)}(z) \tag{44}$$

where $H_\nu^{(1)}$ is the Hankel function of the first kind. The denominator $\eta_\nu(z)$ is given by

$$\eta_\nu(z) = \frac{\partial}{\partial\nu} [h_\nu^{(1)}(z) + z h_\nu^{(1)'}(z)] \tag{45}$$

where prime denotes derivative with respect to z. In (43), ν_m , m=0,1,2 ... are the roots to the transcendental equation

$$(h_\nu^{(1)} + z h_\nu^{(1)'}(z)) \Big|_{\substack{\nu=\nu_0,\nu_1,\nu_2\,\cdots \\ z\,=\,ka}} = 0 \tag{46}$$

as a function of ν. Each term in (43) is a creeping wave. For large ka, Sommerfeld [17] shows that asymptotically

$$\nu_m = ka\,[1 + \tfrac{1}{2}(4m+1)^{2/3}\,(\tfrac{3\pi}{4ka})^{2/3}\,e^{i\,\pi/3}] \tag{47}$$

Since the ν's are large in magnitude, $P_\nu(-\cos\theta)$ can also be approximated

24

by its large argument asymptotic expression e.g. (see [17], p. 149).

$$P_\nu(-\cos\theta) \approx \frac{1}{(2\pi\nu\sin\theta)^{\frac{1}{2}}} \cos\left(\nu+\frac{1}{2}\right)(\pi-\theta) - \pi/4 \qquad (48)$$

provided $|\nu| \gg 1$ and θ not too near 0 or π.

Now the phase change associated with the creeping ray passing through the focus at the poles of the sphere is contained in expression (48) as has been shown by Wait [7]. We use his argument and note that result (48) can be decomposed into two "rays" i.e. we rewrite (48) as

$$P_\nu(-\cos\theta) \approx A\left[e^{i\left(\nu+\frac{1}{2}\right)\theta} + e^{-i\pi/2}e^{i\left(\nu+\frac{1}{2}\right)(2\pi-\theta)}\right] \qquad (49)$$

where

$$A = \frac{e^{-i\left(\nu+\frac{1}{2}\right)\pi}}{2(2\pi\nu\sin\theta)^{\frac{1}{2}}} \qquad , 0 < \theta < \pi$$

The interpretation is that there are two traveling waves on great circle paths. One travels through an arc θ, the other through the arc $(2\pi-\theta)$. Upon going through the focus at $\theta = \pi$, the second ray path picks up a phase advance of $\pi/2$ radians. Although not demonstrated from this argument, the phase advance is not abrupt (see [7]) but continuous, and $P_\nu(-\cos\theta)$ near π is finite i.e.

$$P_\nu(-\cos\theta) \approx J_0\left(\left(\nu+\frac{1}{2}\right)(\pi-\theta)\right) + O((\pi-\theta)^2)$$

$$\theta \approx \pi$$

(see [7], p. 163). This completes our discussion of the $\pi/2$ phase advance

associated with spheroid focus phenomena, and as used in our creeping ray resonance condition(3).

ACKNOWLEDGMENT

REFERENCES

[1] D. G. Dudley, "Parametric Identification of Transient Electromagnetic Systems," Wave Motion, no. 5, North-Holland, pp. 369-384, 1983.

[2] A. Q. Howard, Jr., "A Geometric Theory of Natural Oscillation Frequencies in Exterior Scattering Problems," Air Force Office of Scientific Research Final Report, grant no. 78-3727, also AFWL IN 378.

[3] J. B. Keller and S. I. Rubinow, "Asymptotic Solution of Eigenvalue Problems," Annals of Physics, vol. 9, pp. 24-75, 1960.

[4] E. Heyman and L. B. Felsen, "Creeping Waves and Resonances in Transient Scattering by Smooth Convex Objects," IEEE Trans. Antennas and Propagation, 1984.

[5] H. Bremmer, Terrestrial Radio Waves, Theory of Propagation, Elsevier Publishing Company, New York, N.Y., 1949.

[6] V. A. Fock, Electromagnetic Diffraction and Propagation Problems, ed. A. L. Cullen, V. A. Fock and J. R. Wait, Pergamon Press, London, 1965.

[7] J. R. Wait, Electromagnetic Waves in Stratified Media, sec. ed., Pergamon Press, Oxford, 1970.

[8] N. A. Logan, General Research in Diffraction Theory Report No. LMSD-288087, Missiles and Space Division, Lockheed Aircraft Corporation, 1959.

[9] D. S. Jones, Methods in Electromagnetic Wave Propagation, Oxford Engineering Science Series, Oxford, 1979.

[10] D. J. Struik, Classical Differential Geometry, sec. ed., Adison-Wesley Pub. Co., Reading. Mass., 1961.

[11] F. W. J. Olver, <u>Asymptotics and Special Functions</u>, Academic Press, New York, 1974.

[12] M. A. Leontovich, "Approximate Boundary Conditions for the Electro-magnetic Field on the Surface of a Good Conductor," <u>Investigations on Radiowave Propagation</u>, part II, 5-12, Printing House of the Academy of Sciences, Mowcow, 1948 (Also reprinted Diffraction, Refraction and Reflection of Radio Waves, Ed. N. A. Logan, Antenna Laboratory Air Force Cambridge Research Center, Bedford, Mass., AFCRC-TN-57-102 ASTIA document no. AD117276, 1957).

[13] M. Abramowitz and I. Stegun (editors), <u>Handbook of Mathematical Functions</u>, National Bureau of Standards, Applied Mathematical Series 55, Super-intendent of Documents, U.S. Government Printing Office, Washington, D.C., 1964.

[14] W. Gröbner and N. Hofreiter, <u>Integraltafel; Zweiterteil; Bestimmte Integrale</u>, Vierte Auflage, Springer-Verlag, Wein and New York, 1966.

[15] I. S. Gradshteyn and I. M. Ryzhik, <u>Tables of Integrals, Series and Products</u>, fourth edition, (trans. and ed. A. Jeffrey), Academic Press, New York, 1980.

[16] L. Marin, "Natural-Mode Representation of Transient Scattering From Rotationally Symmetric, Perfectly Conducting Bodies and Numerical Results for a Prolate Spheroid," <u>Air Force Interaction Note 119</u>, Kirtland Air Force Base, Albuquerque, New Mexico, 1972.

[17] M. Born and E. Wolf, <u>Principles of Optics</u>, third ed, Pergamon Press, Oxford, pp. 435-449, 1965.

[18] A. Sommerfeld, <u>Partial Differential Equations in Physics</u>, Academic Press, New York, pp. 279-289, 1949.